

The influence of the thickness of the CdS emitter layer on the performance of a CIGS solar cell with acceptor defects

Demba Diallo, Alain Kassine Ehemba, Amsata Ndiaye, Mouhamadou Mamour Socé, Moustapha Dieng

Abstract— In this work, we simulated a solar cell based on CIGS with simple default acceptor, using software (SCAPS) version 3.302 in order to study certain parameters. In particular, we have varied the thickness of the CdS emitter (0.05 μm , 0.04 μm and 0.03 μm) to study its influence on the performance of the cell. We were able to record that the energy efficiency increased from 16.50% for a thickness of 0.05 μm of the emitter to 16.87% for a thickness of 0.03 μm of the emitter. We also noted an improvement in other parameters, such as the form factor from $\text{FF} = 79.81\%$ to 80.10%, with the decrease in the thickness of the CdS. And from the Nyquist diagram, we also determined parameters like the series resistance to get an idea on the equivalent electrical circuit of the studied cell.

Index Terms— CdS semiconductor, acceptor defects, Cu(In,Ga)Se₂, Nyquist Plot, SCAPS, solar cell.

I. INTRODUCTION

The use of solar energy is made from its thermal and photovoltaic sections. The core of photovoltaic use is the solar cell. We note several types of solar cells, but our research is concentrated on CuInSe₂ thin film solar cells, Cu(In, Ga)Se₂ solar cells and their derivatives. Several publications have been made in the aim to improve the performances of these types of solar cells. [1]

In this work, we simulated on SCAPS 3.302 the influence of the thickness of the CdS layer on the quality of a CIGS solar cell with simple acceptor defects. Different determination methods of electrical parameters have been used on the solar cell. To improve the efficiency of this solar cell, these parameters must be optimized. In addition, a schematic representation of the solar cell in its equivalent circuit [2] can be used to determine electrical parameters, such as series resistances, shunt resistances and photovoltaic capacity. In this work, the impedance spectroscopy method is used for the characterization of solar cells. This method allows us to use the BODE and NYQUIST diagrams [3].

Demba DIALLO is working at the Laboratory of Semiconductors (LASES), Department of Physics, Cheikh Anta Diop University of Dakar. SENEGAL. Research Interests: Physics an Applications, Thin Film Solar Cells

Dr Alain Kassine EHEMBA is working at the Laboratory of Semiconductors (LASES), Department of Physics, Cheikh Anta Diop University of Dakar. SENEGAL. Research Interests: Physics an Applications, Thin Film Solar Cells

Pr Moustapha DIENG is working at the Laboratory of Semiconductors (LASES), Department of Physics, Cheikh Anta Diop University of Dakar. SENEGAL. Research Interests: Physics an Applications, Thin Film Solar Cells. He's the Manager of the research project.

II. THEORY

A. Evaluation of parameters

The adapted structure is essentially composed of an n-p cell based on Cu(In,Ga)Se₂ on which is deposited an n-type CdS layer. A diagram of the structure is illustrated in the Fig. 1 and the Table 1 presents the physical parameters used in the simulation. The choice of these parameters values was taken on the model of some laboratory structures. However, to ensure a good metallic contact on this layer, two different options have been developed. One is to open a window in the ZnO layer and the metal contact is made directly on the CIGS.

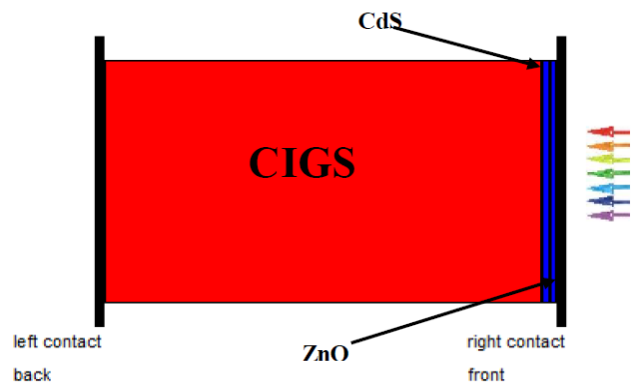


Fig. 1: Structure of the cell.

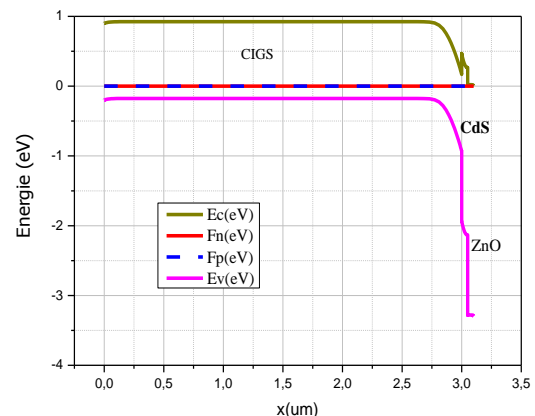


Fig. 2: diagram band of the 1D model used for the simulation.

We note that the structure was studied under illumination AM1.5, with a power of $P=100\text{mW}/\text{cm}^2$, and at room temperature $T = 300 \text{ K}$.

Table. 1

Physical parameters used in the simulation

	ZnO	CdS	CIGS
Thickness (μm)	0.05	0.05	3
Dielectric Constant	9	10	13.6
Electron Mobility ($\text{cm}^2/\text{V.s}$)	10^2	10^2	10^2
Hole Mobility ($\text{cm}^2/\text{V.s}$)	2.5×10^1	2.5×10^1	2.5×10^1
Carrier Density (cm^{-3})	10^{18}	10^{17}	2.10^{16}
bandgap (eV)	3.3	2.4	1.1
N_c (cm^{-3})	2.2×10^{18}	2.2×10^{18}	2.2×10^{18}
N_v (cm^{-3})	1.8×10^{19}	1.8×10^{19}	1.8×10^{19}
Electronic affinity (eV)	4.45	4.2	4.5

B. The Cu(In,Ga)Se₂ absorber layer

In the absorber layer, we have a bandgap of 1.1eV and a doping density of $2 \times 10^{16} \text{ cm}^{-3}$. It has an acceptor-type defect with possible charge states (1-, 0), with a Gaussian energy distribution: $E_t = 0.60 \text{ eV}$ and a characteristic energy of 0.10eV above the Valence band level with a defect density of $1.77 \times 10^{13} \text{ cm}^{-3}$, the capture constants are given in Table 2 [4].

Table 2

Capture constants used for the SCAPS model.

Level of defect	Level (0 / -)
$c_n(\text{cm}^3/\text{s})$	5×10^{-12}
$c_p(\text{cm}^3/\text{s})$	10^{-15}

C. Physics of photovoltaic cells

Most thin-film solar cells consist of several semiconductors separated by different properties. A complete description of the entire device under illumination can be given by the concentration of the carriers at each point in the device. As well as boundary conditions appropriate to interfaces and contacts, it results in a system of equations coupled in (ϕ, n, p) or (ϕ, E_{Fn}, E_{Fp}) . It can be accomplished by uniformly solving all of the following equations, shown here in their dimensional forms:

$$\frac{\partial \phi}{\partial x^2} = -\frac{\partial \xi}{\partial x} = -\frac{\rho}{\epsilon_s} = \frac{q(n - p + N_A - N_D)}{\epsilon_s} \quad (1)$$

$$E_{Fn} = E_i + kT \ln \left(\frac{n}{n_i} \right) \quad (2)$$

$$E_{Fp} = E_i + kT \ln \left(\frac{p}{n_i} \right) \quad (3)$$

In these expressions E_i is the intrinsic Fermi level, $(E_{Fn} - E_{Fp})$ the conduction bands and the valence of the quasi-Fermi levels. The position of the quasi-Fermi levels, under illumination or applied polarization, is mainly determined by the properties of the defect states located in the gap band.

$$J_n = q\mu_n \left(n\xi + \frac{kT}{q} \frac{\partial n}{\partial x} \right) = \mu_n n \frac{\partial F_{Fn}}{\partial x} \quad (4)$$

$$J_p = q\mu_p \left(p\xi + \frac{kT}{q} \frac{\partial p}{\partial x} \right) = \mu_p p \frac{\partial F_{Fp}}{\partial x} \quad (5)$$

In these expressions J_n represents the current density of the electrons, J_p the current density of the holes, μ_n the mobility of the electrons, μ_p the mobility of the holes and ξ the electric field.

The main functionality of SCAPS must solve the dimensional equations of a semiconductor. In the majority of the layers, the constitutive equations are given by equations (4 and 5).

III. RESULTS AND DISCUSSION

A. Current-Voltage characteristic (J-V)

The fig. 3 shows the current-voltage characteristic (J-V) of the solar cell with different thicknesses of the emitter: CdS at 0.05 μm , CdS at 0.04 μm and CdS at 0.03 μm . And the output parameters of Fig. 3 are given in Table 3.

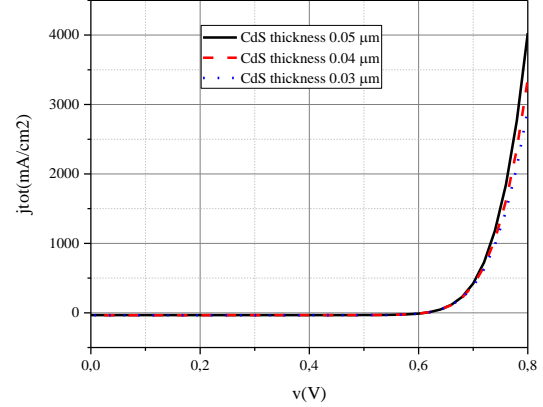


Fig. 3: Current voltage characteristic J (V) of the solar cell with different thicknesses of the emitter layer: CdS at 0.05 μm , CdS at 0.04 μm and CdS at 0.03 μm .

With the decrease in the thickness of the emitter, we notice a small increase in J_{cc} and FF ; however a very slight increase in V_{oc} is also noticed. The conversion efficiency of the cell increases from 16.50% to 16.87%.

This is explained by the fact that the incident photons of short wavelengths of the visible are more sensitive to the change in the thickness of the emitter. Since the emitter is n-type, the increasing in the thickness of this region affects the density of the photo-generated minority carriers that are the holes. The thicker is the region, the better is the recombination of the minority carriers, since they have to travel more distance to reach the junction and are expelled by the field of the depletion zone to reach the region p where they become the majority.

Table 3

Macroscopic electrical parameters of the cell with the effect of the thickness of the transmitter CdS

Thickness CdS (μm)	V_{oc} (V)	J_{cc} (mA/cm^2)	FF (%)	η (%)
0.05	0.6122	33.77	79.81	16.50
0.04	0.6126	34.10	79.94	16.70
0.03	0.6129	34.36	80.10	16.87

B. Capacitance - voltage (C-V) and capacitance - frequency (C-f) Characteristics

The fig. 4 shows the capacitance-voltage characteristic. We see an increase in capacitance with the increase in applied voltage. The capacitance value varies from 41.76 nF/cm² to 285.05 nF/cm² with a thickness of 0.05 μm of the emitter, from 41.44 nF/cm² to 249.13 nF/cm² with a thickness of 0.04 μm of the emitter and 43.07 nF/cm² to 227.04 nF/cm² with a thickness of 0.03 μm of the emitter.

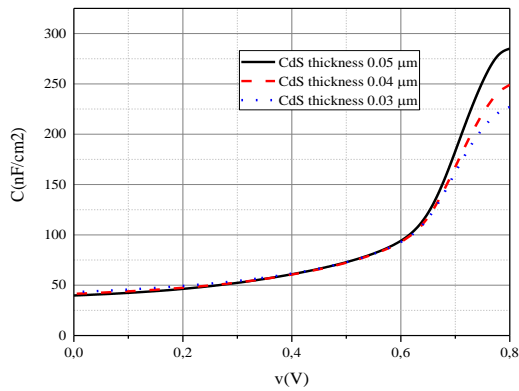


Fig. 4: the curve of variation of the capacitance according to the voltage applied with different thicknesses of the emitter.

The capacitance increases exponentially due to the occupation of the electronic density of states by the excess of minority carriers. The observed variation of the diffusion capacity with the applied voltage indicates the distribution of the electronic state in the bandgap and the displacement of the Fermi level. However, a small change on the majority charge carriers causes a downward movement of the Fermi level of the holes.

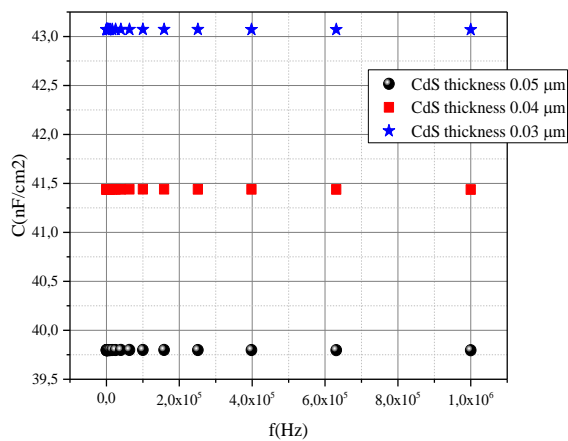


Fig.5: the curve of variation of the capacitance according to the frequency with different thicknesses of the emitter layer.

For the capacitance as a function of the frequency represented in Fig.5, we have an increase in the capacitance with the decrease in the thickness of the CdS. It is 43.1 nF/cm² for 0.03 μm emitter solar cell, 41.4 nF/cm² for 0.04 μm emitter solar cell and 39.8 nF/cm² for a 0.05μm emitter solar cell. We also notice for a constant temperature of 300 K, the capacitance of the samples remains constant. The contribution of a single level of defect to capacity can be described by a relaxation process [5].

$$C(\omega) = C_{hf} + \frac{1}{1 + \omega^2 \tau^2} (C_{lf} - C_{hf}) \quad (6)$$

With C_{hf} the capacity at high and C_{lf} the capacity at low frequency.

C. Conductance-Voltage characteristic (G-V)

The figure 6 shows the variation of the conductance as a function of the applied voltage. We note that the conductance

of the emitter cell 0.05 μm remains higher than that of the emitter cell 0.03 μm.

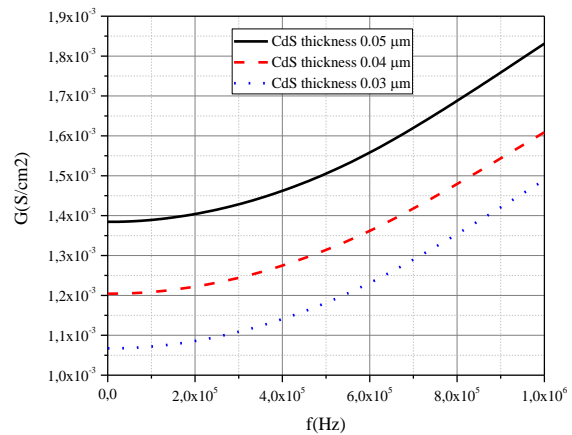


Fig. 6: the conductivity variation curve according to the voltage applied with different thicknesses of the emitter layer.

We can note that the thickness of the emitter doesn't affect too much the conductivity of the cell.

D. Nyquist Plot

The NYQUIST plot consists in representing the imaginary part according to the real part of the impedance (Z) of the solar cell. The measurements were made on the polycrystalline CIGS solar cell under different illumination conditions. The conditions and impedance spectra plotted (fig. 7) in the complex plane (Z_{im}, Z_{re}), are also known as Nyquist name [6-7]. To determine the resistances R_s and R_p, we have plotted a representation of Nyquist which is a

semicircle of center $\begin{pmatrix} R_p + R_s \\ 0 \end{pmatrix}$ and of radius: $\left(\frac{R_p}{2} \right)$

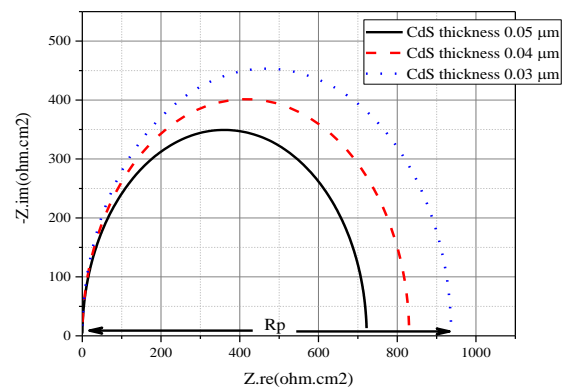


Fig. 7: The impedance spectrum of the CIGS polycrystalline solar cell for different thicknesses of the emitter layer.

Table 4

Values of the parallel resistance according to the thickness of the CdS emitter.

Thickness CdS (μm)	Rp (ohm/cm ²)
0.05	727.47
0.04	832.90
0.03	939.24

According to Table 4, the thickness of the CdS has a strong influence on the electrical parameters such as the series resistance. It passes from 725.47 ohm / cm² for a CdS thickness of 0.05 (μm) to 939.24 ohm / cm² for a CdS thickness of 0.03 (μm). It should be noted that the greater the resistance, the better the quality of the cell studied.

E. Diagram of Bode: Dynamic Impedance Phase

The BODE diagram of the phase of the dynamic impedance gives the evolution of the phase according to the decimal logarithm of the excitation frequency. The Bode diagram provides information about the frequency behavior of a system. The BODE diagram of the phase of the impedance of the photovoltaic cell is given in the Fig.8.

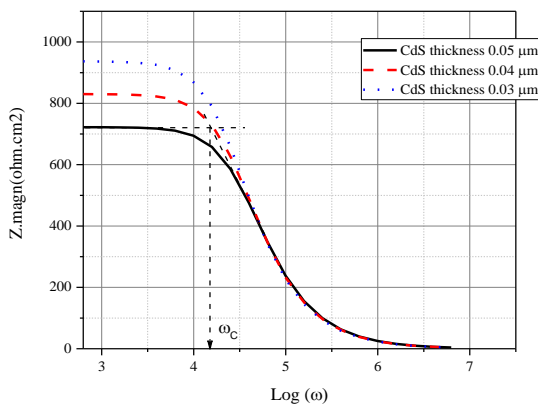


Fig. 8: Modulus of the impedance according to the logarithm of the frequency (ω) for different thicknesses of the emitter.

For the angular frequencies in the interval 0 < ω < ω_c, the module of the dynamic impedance of the solar cell is independent of the frequency. And for the values of the pulsation such that ω > ω_c the modulus of the impedance decreases with the pulse. Thus the intersection of the extensions of the two linear parts of the curve (Fig. 8) makes it possible to obtain the angular cut-off pulsation ω_c [8].

Table 5

Cutoff frequency values as a function of the thickness of the CdS transmitter

Thickness CdS(μm)	Cut-off Pulsation ω _c (rad/s)
0.05	1.29 × 10 ⁴
0.04	1.12 × 10 ⁴
0.03	0.96 × 10 ⁴

According to the Table 5, the lowest cut-off frequency was obtained at a thickness of 0.03 μm. This point is explained by the fact that a defect can only contribute to the capacitance if the angular frequency is sufficiently low.

IV. CONCLUSION

The reduction in the thickness of the emitter of the cell leads to an improvement in the efficiency, although there is the presence of defects in the active layer of the CIGS. We have also noticed the regulation of certain parameters such as the parallel resistance of the equivalent electrical circuit. The

optimization of the thickness of the active layer and the quality of the interfaces are already foreseen.

REFERENCES

- [1] Alain K. Ehemba, Mouhamadou Mamour Soce, Ibrahima Wade, Demba Diallo and Moustapha Dieng "Influence of the use temperature on the Capacitance-Voltage measures and the external quantum efficiency of a Cu (In, Ga)Se₂ thin film solar cell", Pelagia Research Library, 2016, 7(3):187-192.
- [2] R. Anil Kumar, M.S. Suresh and J. Nagaraju IEEE "Transactions on Electron Devices", Vol.48, No.9 September 2001.
- [3] Lathi, Bhagwandas and Pannalal, "SIGNALS, SYSTEMS AND CONTROLS", Intext Educational Publisher, New York (1973-1974).
- [4] Demba Diallo, Moustapha Dieng and Dr. Alain Kassine Ehemba, "Modelling Defects Acceptors And Determination Of Electric Model From The Nyquist Plot And Bode In Thin Film CIGS", INTERNATIONAL JOURNAL OF SCIENTIFIC & TECHNOLOGY RESEARCH VOLUME 4, ISSUE 12, DECEMBER 2015.
- [5] A. Jasenek, U. Rau, V. Nadenau, H.-W. Schock, "Electronic properties of CuGaSe₂-based heterojunction solar cells. Part II. Defect spectroscopy", Journal of Applied Physics, vol. 87, No.1, pp.594-602, 2000.
- [6] S. Kumar, P. K. Singh, G. S. Chilana, S. R. Dhariwal, "Generation and recombination life time measurement in silicon wafers using impedance spectroscopy", Semicond. Sci. Technol. 24 (2009)095001-095008.
- [7] K. Pandey, P. Yadav, I. Mukhopadhyay, "Elucidating different mass flow direction induced polyaniline-ionic liquid interface properties: insight gained from DC voltammetry and impedance spectroscopy", J. Phys. Chem.B.118 (2014)3235-3242.
- [8] M. Ndiaye, Z. Nouhoukoko, I. Zerbo, A. Dieng, F. I. Barro, G. Sissoko, "determination of electrical parameters of a solar cell under illumination with monochromatic frequency modulation, from diagrams of Bode and Nyquist", J. Sci. Vol. 8, N° 3 (2008) 59 -68.



Demba DIALLO is working at the Laboratory of Semiconductors (LASES), Department of Physics, Cheikh Anta Diop University of Dakar. SENEGAL. Research Interests: Physics an Applications, Thin Film Solar Cells.



Dr Alain Kassine EHEMBA is working at the Laboratory of Semiconductors (LASES), Department of Physics, Cheikh Anta Diop University of Dakar. SENEGAL. Research Interests: Physics an Applications, Thin Film Solar Cells.



Pr Moustapha DIENG is working at the Laboratory of Semiconductors (LASES), Department of Physics, Cheikh Anta Diop University of Dakar. SENEGAL. Research Interests: Physics an Applications, Thin Film Solar Cells. He's the Manager of the research project.